

# Molecular Modeling Approaches for the Prediction of the Nonspecific Binding of Drugs to Hepatic Microsomes

Matthew J. Sykes,<sup>\*,†</sup> Michael J. Sorich,<sup>‡</sup> and John O. Miners<sup>†</sup>

Department of Clinical Pharmacology, Flinders University and Flinders Medical Centre, Adelaide, Australia,  
and School of Pharmacy and Medical Sciences, University of South Australia, Adelaide, Australia

Received May 31, 2006

Molecular modeling approaches for the prediction of the nonspecific binding of drugs to hepatic microsomes were examined using a published database of 56 compounds. Models generated were evaluated using an independent test set of 13 compounds. A pharmacophore approach identified structural features of drugs associated with nonspecific binding. A side-chain amino group and complementary hydrophobic domain were the principal features noted. The use of shape overlays, based on the pharmacophore, in conjunction with a chemical force field in the program ROCS, yielded discrimination between molecules classified as strong binders (experimental fraction unbound in microsomes < 0.50) and those with a lower degree of binding (experimental fraction unbound in microsomes > 0.50). In the initial data set of 56 molecules, 18 were classified as strong binders (on the basis of the above criteria), and all of those were recovered in the top 22 molecular hits from ROCS. Additionally, computationally generated values of log *P* were shown to provide a reasonable estimate of the fraction unbound in microsomes, providing the compounds were in their basic form at physiological pH.

## INTRODUCTION

Approaches to predict the drug hepatic clearance and extraction ratio and the magnitude of inhibitory drug interactions in humans have attracted intense interest over the past decade or so, particularly for assessing the pharmacokinetic parameters of newly discovered drugs.<sup>1–4</sup> Experimental strategies adopted typically employ human liver microsomes or human hepatocytes as the enzyme sources to calculate an in vitro intrinsic clearance ( $CL_{int}$ ), which may be extrapolated to hepatic clearance and extraction ratio using a mathematical model for these parameters.<sup>2–5</sup> The measurement of product formation under initial rate conditions allows calculation of the Michaelis constant ( $K_m$ ) and maximal velocity ( $V_{max}$ ) and then  $CL_{int}$  (as  $K_m/V_{max}$ ). Alternatively, the rate of substrate depletion (at a low substrate concentration) may be used to estimate  $CL_{int}$ .<sup>5,6</sup> Similarly, in vitro approaches, based on the measurement of an inhibition constant ( $K_i$ ), provide a basis for determining the extent of an inhibitory drug interaction in vivo.<sup>3,6–10</sup> However, for in vitro data to be of value, measured kinetic parameters must be accurate.

The majority of drugs are lipophilic organic compounds that may bind nonspecifically to components of the incubation mixture,<sup>11–14</sup> presumably predominantly to membrane phospholipids. Indeed, for some drugs, particularly lipophilic bases, nonspecific binding may exceed 90%. Where nonspecific binding occurs, the concentration of free drug present in incubations is reduced, and hence, added concentration is not representative of the drug available to interact with the enzyme active site. Under these circumstances, measured kinetic parameters ( $K_m$ ,  $CL_{int}$ , and  $K_i$ ) underestimate true values, and consequently, hepatic clearance and the magni-

tude of inhibitory drug interactions in vivo are both underpredicted.<sup>11–18</sup>

Correction for nonspecific binding improves the accuracy of extrapolated in vitro kinetic data. Currently available experimental methods for measuring the fraction of drug unbound in the incubation mixture (e.g., equilibrium dialysis, ultrafiltration, and ultracentrifugation) are, however, relatively laborious and time-consuming. To predict nonspecific binding, Austin et al.<sup>19</sup> compiled a database of drugs (comprising organic acids, bases, and neutrals) for which the fraction unbound in microsomal incubations ( $f_{u,mic}$ ) had been reported and investigated the relationship between this parameter and lipophilicity. They reported a linear relationship between  $\log\{(1 - f_{u,mic})/f_{u,mic}\}$  and  $\log P/D$  (viz.,  $\log P$  for bases and  $\log D$  for acids and neutrals) for the combined data set. Despite the highly significant linear relationship ( $R^2 = 0.82$ ), linearity appeared less convincing at  $\log P/D$  values less than 3, and there was no attempt to classify drugs according to charge. Important in this regard is the binding of most bases is generally higher than that of acids and neutrals.<sup>11–13,19</sup>

There is increasing awareness of the importance of computational (in silico) approaches for predicting the absorption, distribution, metabolism, excretion, and toxicity (ADMET) characteristics of new drug candidates.<sup>4,20–21</sup> Potentially, in silico methods permit the calculation of ADMET parameters without recourse to laboratory-based procedures. Thus, computational approaches capable of estimating  $f_{u,mic}$  and providing insights into the physicochemical properties of drugs that confer extensive nonspecific binding assume importance, given the pivotal role of  $f_{u,mic}$  in the accurate calculation of  $CL_{int}$  and  $K_i$ .

In this study, we employed the database of Austin et al.<sup>19</sup> to further explore relationships between  $f_{u,mic}$  and the structural and physicochemical properties of drugs. In particular, the estimation of  $f_{u,mic}$  using  $\log P$  was analyzed

\* Corresponding author fax: +61-8-8204-5114; e-mail: matthew.sykes@flinders.edu.au.

<sup>†</sup> Flinders University and Flinders Medical Centre.

<sup>‡</sup> University of South Australia.

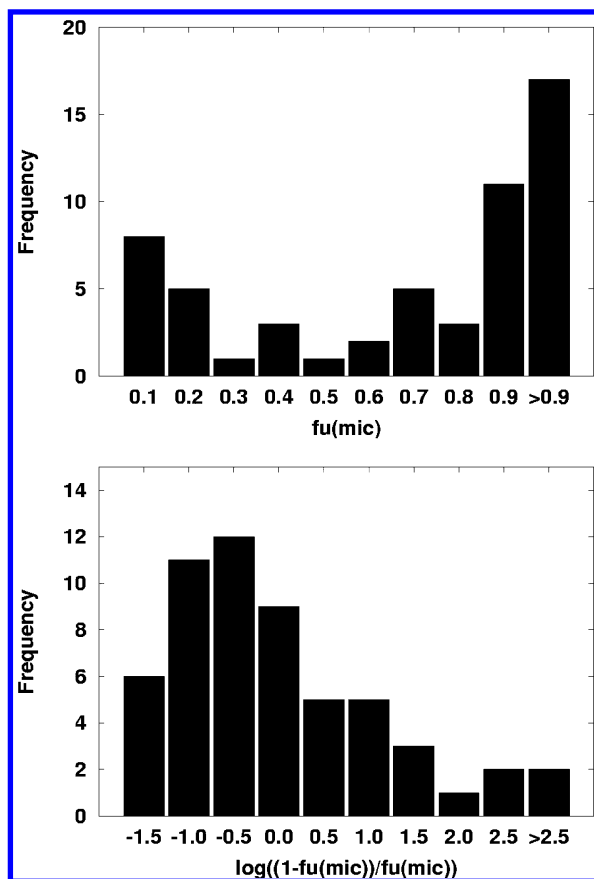


**Figure 1.** Distribution of the 56-compound data set, in terms of  $f_{u,mic}$  (upper panel) and  $\log\{(1 - f_{u,mic})/f_{u,mic}\}$  (lower panel).

in detail, with particular reference to the charge state. In silico values of  $\log P$  were additionally assessed for their predictivity of  $f_{u,mic}$ . Models generated were evaluated using an independent test set of drugs not included in the Austin et al. data set. It was demonstrated that, by utility of a simple pharmacophore model, important structural aspects of extensive microsomal binders were elucidated. Discrimination between stronger microsomal binders and weaker binders was achieved using the pharmacophore in conjunction with shape overlays and a chemical force field.

#### OBJECTIVES

As noted previously, Austin et al.<sup>19</sup> published a method for the prediction of  $f_{u,mic}$ . This was achieved by the use of a transformed  $f_{u,mic}$ , namely,  $\log\{(1 - f_{u,mic})/f_{u,mic}\}$ , which is used because of its similarity to an equilibrium constant. The  $f_{u,mic}$  values of the 56-compound Austin data set did not follow a normal distribution (Figure 1), whereas utilization of the metric  $\log\{(1 - f_{u,mic})/f_{u,mic}\}$  yields a more desirable distribution.

The original Austin et al. approach used experimental  $\log D$  values, together with  $pK_a$ , to obtain an effective “ $\log P/D$ ” value for each molecule under consideration. This is described in detail in the original publication.<sup>19</sup> A linear relationship ( $R^2 = 0.82$ ) was observed between  $\log P/D$  and the transformed  $f_{u,mic}$ .

The objective of the present work was to analyze in depth the data compiled by Austin et al.<sup>19</sup> and to provide further insight into the molecular basis of the nonspecific binding of chemicals to human liver microsomes. The following summarizes the approach adopted:

1. Reanalyze the Austin et al. data, and evaluate the effectiveness of the published model to predict the  $f_{u,mic}$  of the separate three charge classes, namely, acids, bases, and neutrals.

2. Use in silico determined values of  $\log P$  (or other descriptors) as a substitute for experimental  $\log P/D$  to ascertain if computationally derived values yield meaningful correlations with the transformed  $f_{u,mic}$ .

3. Perform a structural analysis of the Austin et al. database, and determine the chemical and structural features which are important for compounds which have “significant” binding (defined as  $f_{u,mic} < 0.5$ ) to the microsomal membrane.

4. Re-evaluate models 2–3 using an independent set of compounds.

#### LOG $P/D$ MODEL AND CHARGE STATE

The Austin data set<sup>19</sup> consisted of experimental values of  $f_{u,mic}$  and  $\log D_{7.4}$ , most of which were measured in the author’s laboratory, but some of the data set was obtained from the published studies of Obach.<sup>11,12</sup> The data set contained 56 compounds, comprising 17 acids, 19 neutrals, and 20 bases. It should be noted that the definition of an acid used by Austin et al. was a  $pK_a$  for the formation of an anion of  $<7.4$ , and that of bases as having a  $pK_a$  for formation of a cation of  $>7.4$ . The same criteria were applied in the current study. The  $f_{u,mic}$  values generated by Austin et al. were determined at pH 7.4 for a drug concentration of 1  $\mu M$ , with rat liver microsomes (1 mg/mL).<sup>19</sup> The measurements of  $f_{u,mic}$  by Obach<sup>11,12</sup> were determined at various protein concentrations (human or rat liver microsomes), all of which were converted to 1 mg/mL using the expression derived in the original paper.<sup>19</sup> The Austin et al. database was augmented here with 13 additional compounds; data obtained from three papers<sup>12,22–23</sup> comprised the test set.

Two structural databases were generated; the first data set contained a single conformer for each molecule, and the second contained a multiconformer database limited to a maximum of 50 conformers per molecule. Default settings in Omega were used unless otherwise specified. The conformers were generated using the Omega program from Openeye software, version 1.8.1.<sup>24</sup> Omega has been shown previously to perform well with respect to producing conformations of protein-bound ligands.<sup>25–26</sup>

Omega first generates a single 3D conformation from the molecule’s connection table on the basis of a random distance-geometry method.<sup>24</sup> The solutions derived using this method are then refined using the Merck molecular force field. The second part of the procedure involves a torsion-driving mechanism based on the initial single molecule solution. Omega uses a depth-first divide-and-conquer procedure to break the molecule into small fragments and generate conformations based on rules in a torsion library.<sup>24</sup> The generated conformers are limited by their total energy as measured by the Dreiding force field.<sup>24</sup> The user can define an appropriate energy window, if desired. For further information, the reader is referred to a recently published article concerning Omega.<sup>27</sup> The article gives an overview of many of the parameters that can be set in Omega, as well as a comparative study of the merits of Omega and the conformer generation module in Catalyst.<sup>28–29</sup>

Compounds were classified into two groups: those with a fraction unbound in microsomes greater than 0.5 (“nonbind-

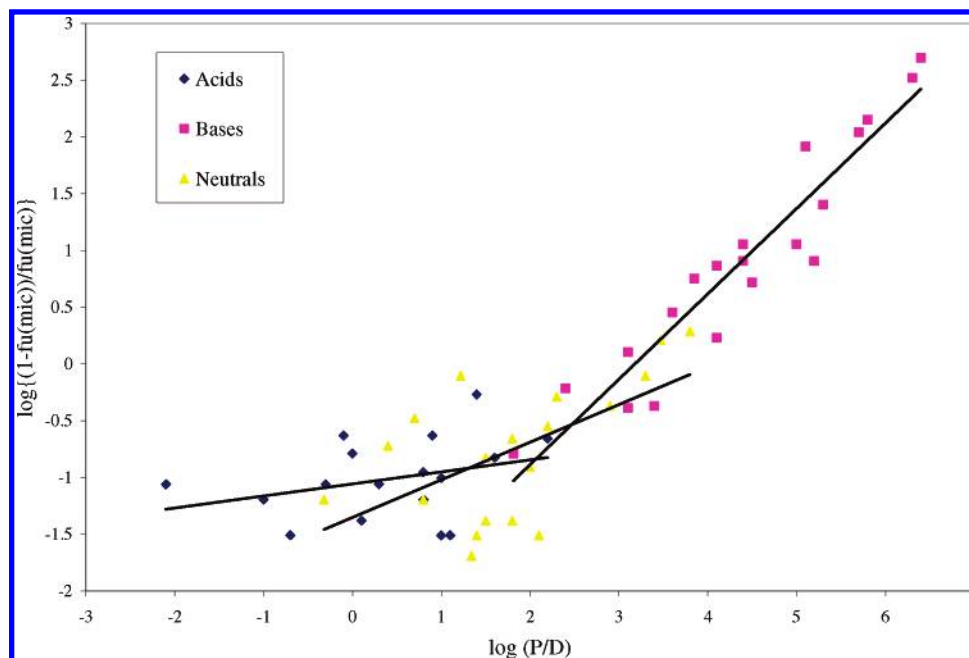


**Figure 2.** The Austin et al. log  $P/D$  model, showing the separate correlations for acids, bases, and neutrals.

ers”) and those with a fraction unbound less than 0.5 (“binders”). If the nonspecific binding phenomenon is not accounted for, a  $f_{u,mic}$  of less than 0.5 corresponds to a 2-fold or greater error in free concentration and, hence, in the estimation of microsomal intrinsic clearance. Given the variability in the prediction of  $CL_{int}$  from microsomal kinetic data, it is generally considered that  $f_{u,mic}$  values greater than 0.5 will not result in the misclassification of in vivo  $CL_H$  (predicted).

When the method developed by Austin et al. is used to predict the transformed  $f_{u,mic}$ , the coefficient of determination ( $R^2$ ) is 0.82. It should be noted that Austin et al. excluded compounds with a  $f_{u,mic} > 0.90$ , on the basis of these compounds having been difficult to discriminate using equilibrium dialysis. This reduces the number of compounds from the original 56 to 37. In this work, we prefer to include these compounds, as ultimately a predictive method must be able to successfully deal with all compounds. If all compounds are included in the Austin log  $P/D$  analysis, the  $R^2$  value drops to 0.77. This plot is shown in Figure 2, with the acids, bases, and neutrals indicated separately. The bases clearly correlate well with the transformed  $f_{u,mic}$ , but the model is less predictive for neutrals and acids.

Lines of best fit to each class are given by the following:

Bases:  $N = 20$ ,  $R^2 = 0.90$ ,  $p < 0.001$ ,  $y = 0.7519x - 2.3902$

Neutrals:  $N = 19$ ,  $R^2 = 0.34$ ,  $p = 0.009$ ,  $y = 0.3315x - 1.3529$

Acids:  $N = 17$ ,  $R^2 = 0.10$ ,  $p = 0.216$ ,  $y = 0.1061x - 1.0579$  where  $N$  is the number of compounds in each class. A value of  $p < 0.05$  was taken as statistical significance.

The standard error of the slope of the three lines of best fit ranges from 7% for the bases, to 33% for the neutrals, and 80% for the acids. Thus, the performance of the model is highly dependent on the charge class.

#### IN SILICO APPROACHES

In this study, we evaluated computational values of log  $P$  from two sources for their predictivity of the transformed

$f_{u,mic}$ , namely, the programs Marvin and SciFinder Scholar 2006.<sup>29,30</sup> Marvin contains a log  $P$  module that can be accessed from a GUI. Additionally, Marvin has a  $pK_a$  calculation program which determines the speciation of a given compound over the full range of pH. SciFinder Scholar 2006 contains log  $P$  values (among other properties) for all compounds in its CAS registry. log  $P$  values are tabulated in a substance information window after completing a substance search. It should be noted that the values of log  $P$  in SciFinder are calculated using the log  $P$  prediction algorithm of ACD software.<sup>31</sup>

In evaluating the performance of the two sources of log  $P$ , the SciFinder values yielded superior predictivity of the transformed  $f_{u,mic}$ . The SciFinder log  $P$  values ( $R^2 = 0.88$ ) were found to correlate better with the experimental log  $P/D$  of Austin et al. than the Marvin calculated values ( $R^2 = 0.77$ ). Thus, the log  $P$  values used throughout this work are those derived using SciFinder and are tabulated in the Supporting Information.

As was the case for the experimentally derived log  $P/D$  values, the bases clearly correlate well with the transformed  $f_{u,mic}$ , but the model is not predictive for neutrals and acids (Figure 3).

Lines of best fit to each class are given by the following:

Bases:  $N = 20$ ,  $R^2 = 0.84$ ,  $p < 0.001$ ,  $y = 0.5738x - 1.8873$

Neutrals:  $N = 19$ ,  $R^2 = 0.38$ ,  $p = 0.004$ ,  $y = 0.3644x - 1.4963$

Acids:  $N = 17$ ,  $R^2 = 0.18$ ,  $p = 0.090$ ,  $y = 0.1172x - 1.3347$  where  $N$  is the number of compounds in each class. A value of  $p < 0.05$  was taken as statistical significance.

To further test the utility of in silico log  $P$  values as a predictor of microsomal binding, an additional set of 13 compounds were obtained from literature searches.<sup>12,22–23</sup> log  $P$  values were obtained from SciFinder Scholar as described earlier and are tabulated in the Supporting Information. Figure 4 shows the data from Figure 3, together with the test set compounds.

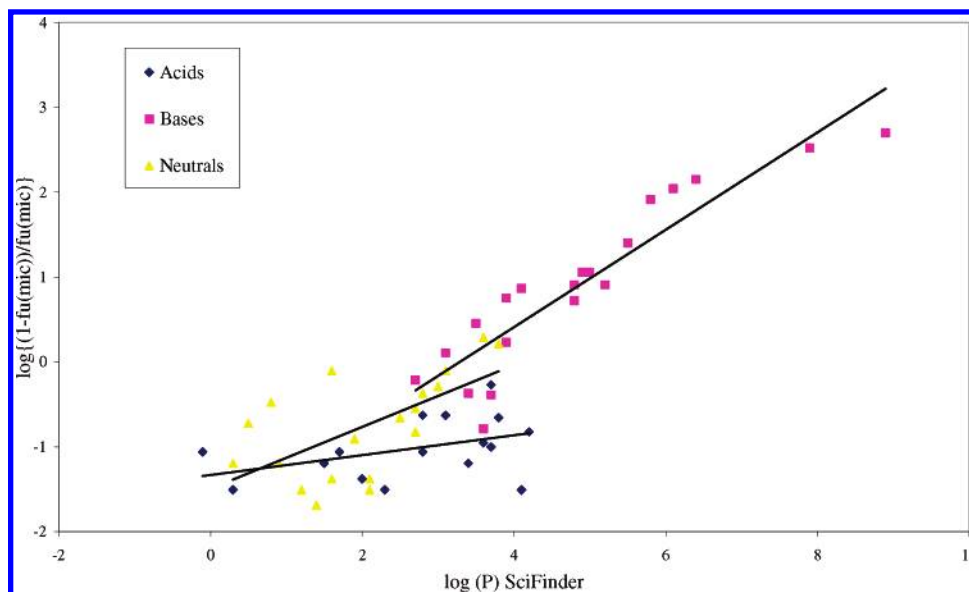


Figure 3. SciFinder log  $P$  predictions, showing the breakdown of the correlation into acids, bases, and neutrals.

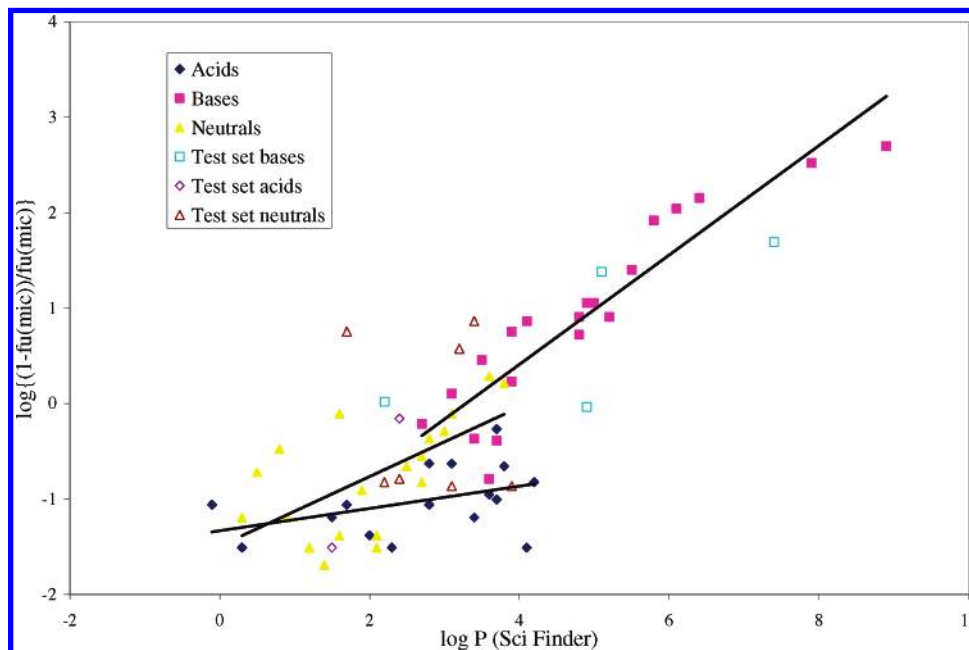


Figure 4. SciFinder log  $P$  predictions, showing the breakdown of separate correlations for acids, bases, and neutrals, as in Figure 3. The 13 molecules comprising the test set are plotted separately.

The addition of the test set compounds further reinforced the earlier observation of log  $P$  being reasonably predictive for bases. The four bases in the test set were predicted with a mean error of 0.65 log units. The acids, and particularly the neutral compounds, have significant scatter. Undoubtedly, the addition of further compounds to this correlation would be of utility in further refining these findings. However, it is clear from all of the models that the log  $P$  methods are only reliably predictive for bases.

#### STRUCTURAL ANALYSIS

We wished to analyze the structural features of the compounds contained within the Austin et al. data set. One of the fundamental principles of chemoinformatics is the so-called similar property principle. This notion is based upon the assumption that structurally similar molecules will have similar biological activity. The objective here was to attempt to separate compounds in the Austin et al. data set into

“binders” and “nonbinders” based upon chemical/structural similarity metrics.

The first approach used the program ROCS from Openeye software.<sup>32</sup> ROCS is a shape-comparison program that uses the simple, but effective, concept of volume overlap as a measure of similarity. This in itself can be useful, for example, to obtain molecules with similar shape to a lead compound. ROCS is particularly effective at searching corporate databases because of its use of smooth Gaussian functions to represent the volume overlap.<sup>33</sup> However, drugs which strongly bind to the microsomal membrane may well share similar chemical characteristics (not necessarily similar shape). ROCS has an additional optimization that can be performed, namely, an in-built color force field. The color force field is used to measure chemical complementarity and to refine shape-based overlays on the basis of chemical similarity. The color force field is constructed as a series of



SMARTS patterns. Types generally defined include hydrogen-bond donors, hydrogen-bond acceptors, hydrophobes, anions, cations, and rings.<sup>32</sup> These are some of the attributes that would be envisaged to be similar between molecules that strongly bind to the microsomal membrane. Further information on aspects of the color force field can be found in the ROCS documentation.<sup>32</sup>

Initially, we used the ImplicitMillsDean color force field in ROCS, which includes a  $pK_a$  model which assumes  $pH = 7$ .<sup>32</sup> ROCS requires the choice of a query compound, which can subsequently be overlaid with the entire data set in order to calculate both a shape match and a color match. First, the shape overlay is performed with the chosen query molecule, and subsequently, the color force field refines the shape-based overlay. Both aspects use a Tanimoto metric of similarity, which yields a score between 0 and 1, with 1 indicating a perfect match. The shape and color indices can be either considered separately or combined to yield a "combination score", which is a straightforward sum of shape and color, yielding a perfect match score of 2.

In this study, the color score itself was found to be of the greatest utility. It should be noted that the method involves the overlay of a single conformer of chlorpromazine with every conformer in the multiconformer database. An optimum ROCS color score is computed for each conformer overlaid, and subsequently, for each molecule, the "hit" chosen is the conformer with the highest color score for that molecule.

#### COLOR FORCE FIELD ANALYSIS

Various molecules with a low fraction unbound value were chosen and tested as the query molecule. After computational experimentation, it was found that the utility of chlorpromazine, which has a fraction unbound of 0.11, as the query molecule gave a high degree of discrimination between "binders" and "nonbinders". It was also noted that the multiconformer data set separated into "binders" and "nonbinders" more effectively than the single conformer database. This is to be expected, as many of the molecules in the data set have a large number of rotatable bonds and, hence, occupy a large conformational space. Verapamil, for example, has 13 rotatable bonds. Additionally, a solvation potential was added, but this did little to affect the results and so was omitted.

An initial orientation is chosen on the basis of inertial properties but may not always be the best choice. Thus, the "randomstarts" option in ROCS was used to alleviate problems that may occur because of the query and database molecules being of substantially different sizes. The "randomstarts" parameter was set to be equal to 50, but in practice, a value of 10 yielded similar results.

Table 1 shows the results of the ROCS analysis, ranking the compounds by their color scores. In each case, the best match of each multiconformer database member molecule is shown. Molecules that are "binders" are shown in bold. It is evident that the "binders" cluster almost exclusively toward the top of the rankings by color score. Some of the close hits to chlorpromazine are intuitive. There are a number of tricyclic compounds (antidepressants) that have common structural features to chlorpromazine. However, several compounds with quite disparate chemical features have high color scores. Examples are shown in Figure 5.

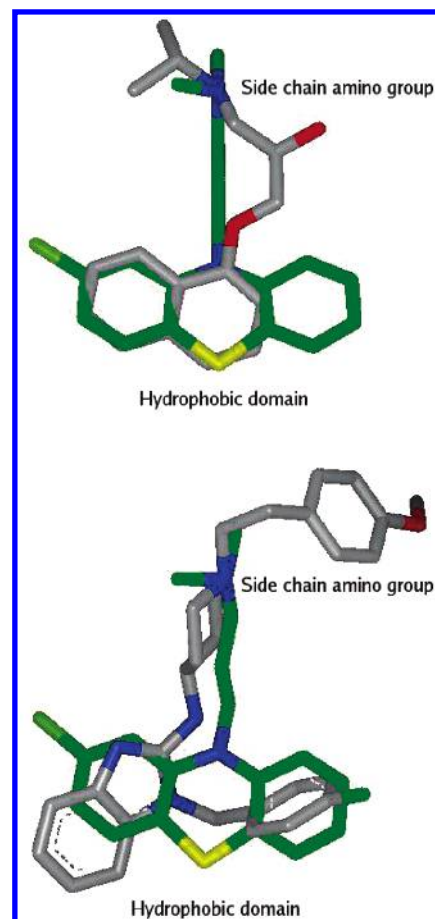


**Figure 5.** Examples illustrating the combined shape/color overlay from the ROCS program. In each case, the query molecule, chlorpromazine, is shown in green. The top image shows propranolol (color score = 0.79), and the bottom image shows astemizole (color score = 0.61).

It is readily apparent that all of the "binders" have a common structural feature in their overlays with chlorpromazine. A side-chain positively charged amino group and hydrophobic domain appear to be the critical structural features present in "binders". In almost all of the "binders", the amino group is protonated at  $pH 7.4$ , as predicted by speciation software.<sup>29</sup> It has been noted previously that the amino group could potentially be a structural motif of relevance when considering the partitioning of drug compounds into phospholipid bilayers.<sup>34</sup> Phospholipid bilayers generally consist of a negatively charged phosphate headgroup and hydrophobic "tails". Thus, it is apparent that the positively charged amino group of the drug molecules can electrostatically interact favorably with the headgroups and the hydrophobic domain with the hydrocarbon lipid tails.<sup>35–36</sup>

The only two molecules that have the charged nitrogen motif and hydrophobic domain, but fail to show strong binding to the microsomal membrane, are diphenhydramine and diltiazem. By inspection, diphenhydramine is a relatively small molecule, having a molecular weight of 255, and may not have a large enough hydrophobic domain to assist in nonspecific binding. Diltiazem, on the other hand, has a relatively large polar surface area, which will unfavorably interact with the hydrophobic core of the bilayer, thus counteracting the effectiveness of the charged amino portion of the molecule interacting with the phospholipid headgroup.

**Table 1.** ROCS Results, Sorted by Scaled Color Tanimoto Value, from Highest to Lowest<sup>a</sup>

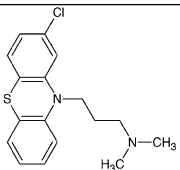
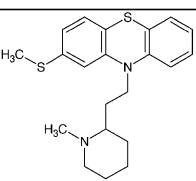
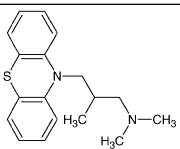
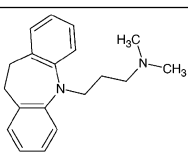
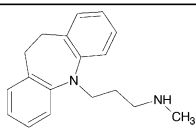
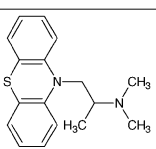
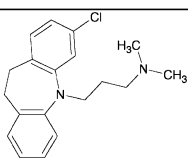
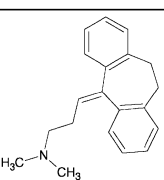
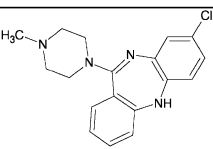
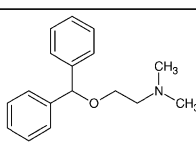
Drug	Structure (shown as neutral species)	Category	Color	Shape	fu <sub>mic</sub>
Chlorpromazine		Base	1.00	1.00	0.110
Thioridazine		Base	1.00	0.85	0.009
Trimeprazine		Base	0.98	0.64	0.081
Imipramine		Base	0.97	0.84	0.160
Desipramine		Base	0.97	0.85	0.120
Promethazine		Base	0.96	0.82	0.110
Clomipramine		Base	0.95	0.82	0.038
Amitriptyline		Base	0.89	0.74	0.081
Clozapine		Base	0.84	0.56	0.260
Diphenhydramine		Base	0.79	0.77	0.710

Table 1. (Continued)

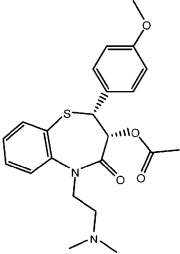
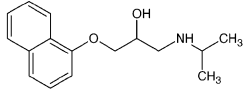
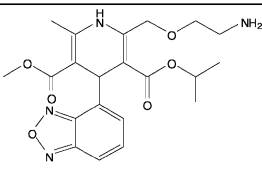
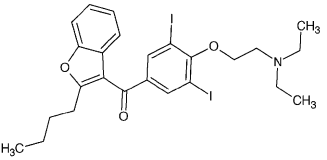
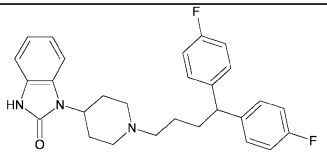
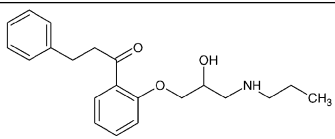
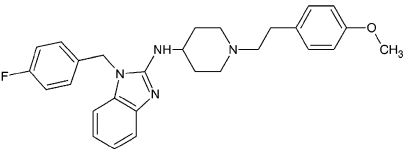
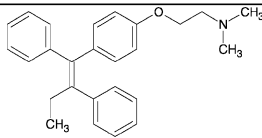
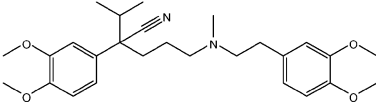
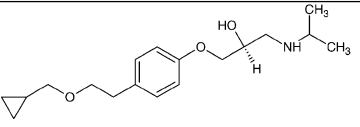
Diltiazem		Base	0.79	0.56	0.860
Propranolol		Base	0.79	0.43	0.440
Isradipine		Neutral	0.76	0.42	0.340
Amiodarone		Base	0.74	0.43	0.002
Pimozide		Base	0.71	0.42	0.007
Propafenone		Base	0.69	0.47	0.150
Astemizole		Base	0.61	0.42	0.012
Tamoxifen		Base	0.61	0.39	0.003
Verapamil		Base	0.60	0.39	0.370
Betaxolol		Base	0.60	0.27	0.620

Table 1. (Continued)

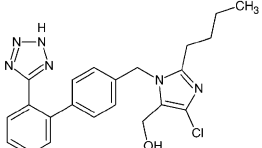
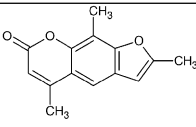
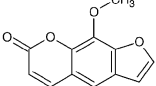
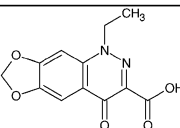
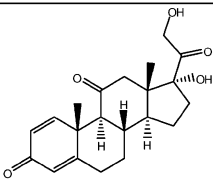
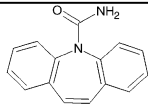
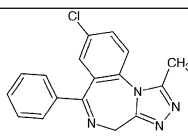
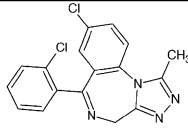
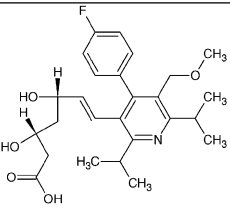
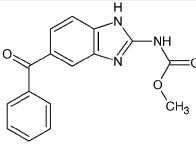
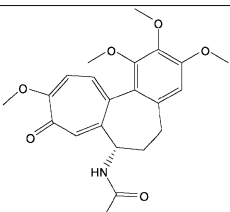
Losartan		Acid	0.58	0.45	0.900
Trioxsalen		Neutral	0.56	0.72	0.380
Methoxsalen		Neutral	0.56	0.68	0.89
Cinoxacin		Acid	0.56	0.60	0.92
Prednisone		Neutral	0.55	0.43	0.56
Carbamazepine		Neutral	0.54	0.76	0.87
Alprazolam		Neutral	0.53	0.59	0.82
Triazolam		Neutral	0.53	0.57	0.78
Cerivastatin		Acid	0.53	0.39	0.65
Mebendazole		Neutral	0.48	0.38	0.70
Colchicine		Neutral	0.44	0.52	0.94



Table 1. (Continued)

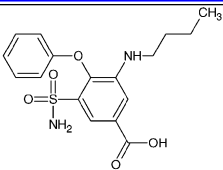
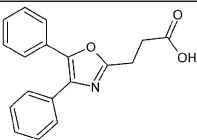
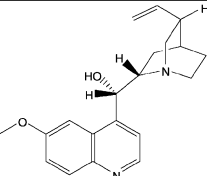
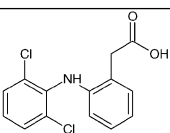
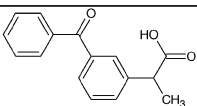
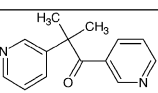
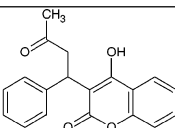
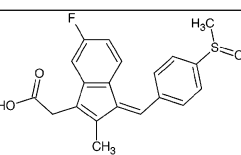
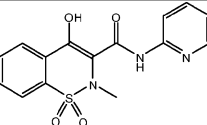
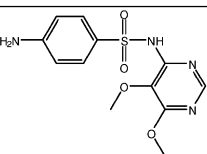
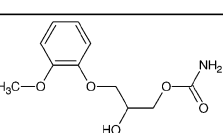
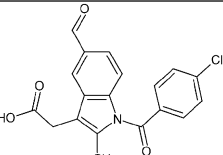
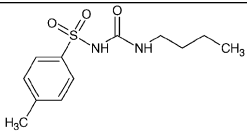
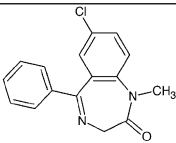
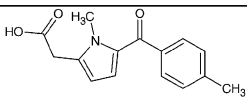
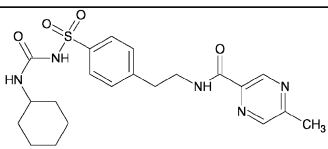
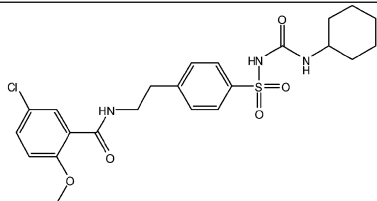
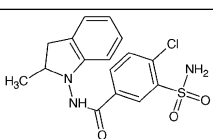
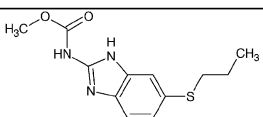
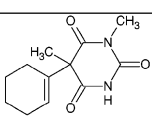
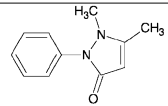
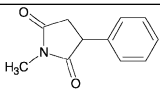
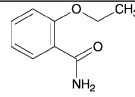
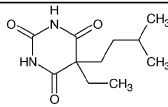
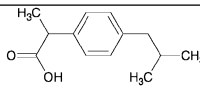
Bumetanide		Acid	0.41	0.45	0.92
Oxaprozin		Acid	0.40	0.70	0.87
Quinidine		Base	0.40	0.66	0.70
Diclofenac		Acid	0.40	0.60	0.97
Ketoprofen		Acid	0.40	0.60	0.92
Metyrapone		Neutral	0.40	0.57	0.97
Warfarin		Acid	0.40	0.56	0.94
Sulindac		Acid	0.40	0.56	0.86
Piroxicam		Acid	0.40	0.53	0.92
Sulfadoxine		Acid	0.40	0.53	0.97
Methocarbamol		Neutral	0.40	0.49	0.84
Indomethacin		Acid	0.40	0.49	0.81

Table 1. (Continued)

Tolbutamide		Acid	0.40	0.48	0.97
Diazepam		Neutral	0.40	0.45	0.66
Tolmetin		Acid	0.40	0.43	0.94
Glipizide		Acid	0.40	0.29	0.96
Glyburide		Acid	0.40	0.27	0.82
Indapamide		Neutral	0.39	0.32	0.96
Albendazole		Neutral	0.38	0.48	0.56
Hexobarbital		Neutral	0.33	0.51	0.96
Dichloralphenazone		Neutral	0.31	0.57	0.94
Phensuximide		Neutral	0.29	0.57	0.75
2-Ethoxybenzamide		Neutral	0.21	0.52	0.98
Amobarbital		Neutral	0.20	0.64	0.97
Ibuprofen		Acid	0.20	0.36	0.91

<sup>a</sup> Chlorpromazine was used as the query molecule. The matches in bold are molecules classified as “binders”, i.e., they have  $f_{u_{mic}} < 0.5$ . The binders clearly cluster toward the top of the table.

Table 2. Test Set ROCS Results, Sorted by Scaled Color Tanimoto Value, from Highest to Lowest<sup>a</sup>

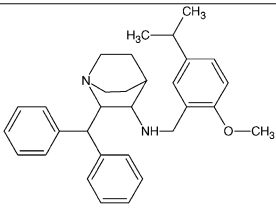
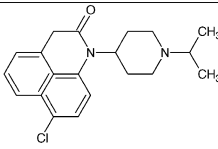
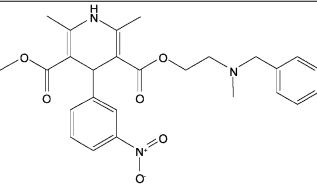
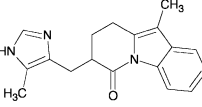
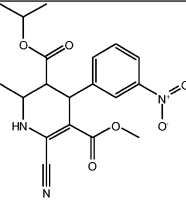
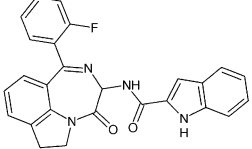
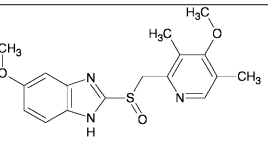
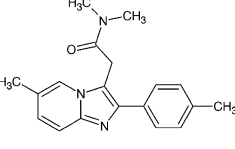
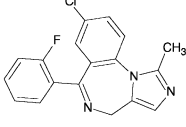
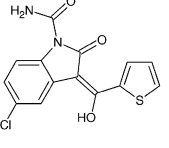
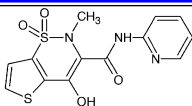
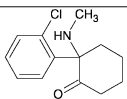
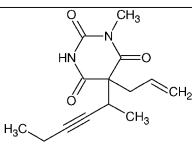
Molecule	Structure (shown as neutral species)	Category	Color	Shape	fu <sub>mic</sub>
Ezlopitant		Base	0.79	0.41	0.02
Lorcainide		Base	0.72	0.54	0.52
Nicardipine		Base	0.71	0.44	0.04
FK1052		Neutral	0.65	0.64	0.21
Nilvadipine		Neutral	0.59	0.37	0.15
FK 480		Neutral	0.57	0.40	0.12
Omeprazole		Neutral	0.56	0.56	0.87
Zolpidem		Neutral	0.43	0.53	0.88
Midazolam		Neutral	0.43	0.60	0.88
Tenidap		Acid	0.40	0.55	0.59

Table 2. (Continued)

Tenoxicam		Acid	0.40	0.47	0.97
Ketamine		Base	<b>0.36</b>	<b>0.61</b>	<b>0.49</b>
Methohexital		Neutral	0.20	0.62	0.86

<sup>a</sup> Chlorpromazine was used as the query molecule but is omitted from the table. The matches in bold are molecules classified as “binders” ( $f_{\text{mic}} < 0.5$ ).

A further important aspect of the side-chain amino group is its geometrical location within the molecule. It was noted by inspection that the charged amino group was located on a flexible side chain usually several angstroms from a hydrophobic ring (or more usually rings; Figure 5). The mean distance between the protonated nitrogen and the nearest ring junction was calculated to be  $4.3 \pm 0.5$  Å for the relevant molecules in the database of Austin et al.<sup>19</sup> It should be noted that, if the charged nitrogen is on a ring, the ring junction chosen is the next adjacent ring. The implications of this preferred location for the charged nitrogen seem to be as follows: (1) isolation of the charged amino group from a more hydrophobic (and generally less flexible) portion of the molecule, (2) creation of two major binding domains, the first involving electrostatic interactions between the charged amino group and the phospholipid headgroups and the second representing hydrophobic interactions between bulky rings and phospholipid tails, and (3) flexibility in the side chain confers a greater range of binding possibilities within the membrane.

The principal aspect to note is that the pharmacophore approach is very good at separating the extensive microsomal binders from the more weakly bound compounds. Thus, it is predicted that the method presented here would work well as a database screening tool. The approach would seem appropriate in selecting compounds that may cause problems with in vitro kinetic studies because of extensive microsomal binding. The concept of a structural motif is also a chemically intuitive idea and is easily rationalized with respect to the structure of the microsomal membrane.

#### EVALUATION OF THE TEST SET

The test set comprised 13 additional compounds, two of which were acids, four were bases, and the remaining seven were neutrals. It should be noted that FK1052 and methohexital are classified here as neutral, but both compounds have a predicted  $pK_a$  close to 7.4. Hence, depending on the method used to predict the  $pK_a$ , these compounds may be classified otherwise. Marvin has been used as the classifier for the charge states of all compounds,<sup>29</sup> as indicated earlier. Fraction unbound data have been converted to 1 mg/mL microsome concentration where necessary, according to Austin et al.<sup>19</sup> An identical analysis to the Austin data set

was applied to the test set. Color scores using chlorpromazine as the query molecule were computed and are presented in Table 2.

The pharmacophore approach performs well overall with respect to the test set. The stronger binders, ezlopitant, nicardipine, FK1052, nilvadipine, and FK480, all have color scores of 0.57 or greater. Lorcainide has a high color score of 0.72 but is classified as a “nonbinder” because it has a fraction unbound of 0.52. The fraction unbound of 0.52 is close to the threshold value of 0.50 and so is a borderline compound in terms of its binding properties.

The main anomaly apparent in Table 2 is the presence of the “binder” ketamine toward the lower end of the table, with a poor color score of 0.36. This compound only just falls into the “binders” category as it has a fraction unbound of 0.49. The extent of binding is perhaps surprising as ketamine has a  $\log P$  of 2.1,<sup>12</sup> which is the same as compounds such as indapamide and amobarbital, which have fraction unbound values of 0.96 and 0.97, respectively.<sup>19</sup> On the other hand, ketamine is a base and is predicted to have a positively charged nitrogen at pH 7.4, which fits well with the proposed pharmacophore. Ketamine has a lower molecular weight than all of the other binders (238 g/mol). Thus, the color score may be lower because there are less pharmacophore features to match. Presumably, the charged nitrogen is dominating binding in the case of ketamine.

#### CONCLUSIONS

Although there are some exceptions to the pharmacophore presented here, the simplicity of the approach, and its intuitive nature, make the technique a robust and rapid aide in the search of large databases. Importantly, the approach is essentially equivalent to a one-variable QSAR method, because the color score resultant from the overlay of a database molecule with chlorpromazine is the sole descriptor. It is likely that the method can be further refined by altering the pharmacophore marginally, or by customizing the definition of the chemical force field to weight the optimization in a more highly tuned manner. As indicated earlier, the chemical force field is comprised of a number of facets such as rings, hydrophobes, anions, cations, and so forth. The force field has in-built default settings or can be customized by the user, by the use of SMARTS patterns. Additionally, a

weighting can be applied to these settings, allowing the force field to be applied with different emphasis. This is one potential way forward in seeking a refinement of the pharmacophore-based method. We intend to examine this in more detail and apply the approach to further experimental work on a larger range of compounds.

# ACKNOWLEDGMENT

Grant support from the National Health and Medical Research Council of Australia is gratefully acknowledged.

**Supporting Information Available:** The log *P* values calculated using SciFinder Scholar are tabulated for all compounds (Austin et al. database and test set). This material is available free of charge via the Internet at pubs.acs.org.

# REFERENCES AND NOTES

- Rodrigues, A. D. Use of in Vitro Human Metabolism Studies in Drug Development. An Industrial Perspective. *Biochem. Pharmacol.* **1994**, *48*, 2147–2156.
- Lavé, T.; Coassolo, P.; Reigner, B. Prediction of Hepatic Metabolic Clearance Based on Interspecies Allometric Scaling Techniques and in Vitro–in Vivo Correlations. *Clin. Pharmacokinet.* **1999**, *36*, 211–231.
- Ito, K.; Iwatsubo, T.; Kanamitsu, S.; Nakajima, Y.; Sugiyama, Y. Quantitative Prediction of in Vivo Drug Clearance and Drug Interactions from in Vitro Data on Metabolism, Together with Binding and Transport. *Annu. Rev. Pharmacol. Toxicol.* **1998**, *38*, 461–499.
- Miners, J. O.; Smith, P. A.; Sorich, M. J.; McKinnon, R. A.; Mackenzie, P. I. Predicting Human Drug Glucuronidation Parameters: Application of in Vitro and in Silico Modeling Approaches. *Annu. Rev. Pharmacol. Toxicol.* **2004**, *44*, 1–25.
- Houston, J. B. Utility of in Vitro Drug Metabolism Data in Predicting in Vivo Metabolic Clearance. *Biochem. Pharmacol.* **1994**, *47*, 1469–1479.
- Miners, J. O.; Knights, K. M.; Houston, J. B.; Mackenzie, P. I. In Vitro–in Vivo Correlation for Drugs and Other Compounds Eliminated by Glucuronidation in Humans: Pitfalls and Promises. *Biochem. Pharmacol.* **2006**, *71*, 1531–1539.
- Von Moltke, L. L.; Greenblatt, D. J.; Schmider, J.; Wright, C. E.; Harmatz, J. S.; Shader, R. I. In Vitro Approaches to Predicting Drug Interactions in Vivo. *Biochem. Pharmacol.* **1998**, *55*, 113–122.
- Ito, K.; Brown, H. S.; Houston, J. B. Database Analyses for the Prediction of in vivo Drug–Drug Interactions from in vitro Data. *Br. J. Clin. Pharmacol.* **2004**, *57*, 473–486.
- Polasek, T. M.; Miners, J. O. Quantitative Prediction of Macrolide Drug–Drug Interaction Potential from in Vitro Studies using Testosterone as the Human Cytochrome P4503A Substrate. *Eur. J. Clin. Pharmacol.* **2006**, *62*, 203–208.
- Uchaipichat, V.; Winner, L. K.; Mackenzie, P. I.; Elliot, D. J.; Williams, J. A.; Miners, J. O. Quantitative Prediction of in Vivo Inhibitory Interactions Involving Glucuronidated Drugs from in Vitro Data: The Effect of Fluconazole on Zidovudine Glucuronidation. *Br. J. Clin. Pharmacol.* **2006**, *61*, 427–439.
- Obach, R. S. Nonspecific Binding to Microsomes: Impact on Scale-Up of in Vitro Intrinsic Clearance to Hepatic Clearance as Assessed through Examination of Warfarin, Imipramine and Propranolol. *Drug Metab. Dispos.* **1997**, *25*, 1359–1369.
- Obach, R. S. Prediction of Human Clearance of Twenty Nine Drugs from Hepatic Microsomal Clearance Data: An Examination of in Vitro Half-Life Approach and Non-Specific Binding to Microsomes. *Drug Metab. Dispos.* **1999**, *27*, 1350–1359.
- McLure, J. A.; Miners, J. O.; Birkett, D. J. Nonspecific Binding of Drugs to Human Liver Microsomes. *Br. J. Clin. Pharmacol.* **2000**, *49*, 453–461.
- Venkatakrishnan, K.; Von Moltke, L. L.; Obach, R. S.; Greenblatt, D. J. Microsomal Binding of Amitriptyline: Effect on Estimation of Enzyme Kinetic Parameters in Vitro. *J. Pharmacol. Exp. Ther.* **2000**, *293*, 343–350.
- Kalvass, J. C.; Tess, D. A.; Giragossian, C.; Linhares, M. C.; Maurer, T. S. Influence of Microsomal Concentration on Apparent Intrinsic Clearance: Implications for Scaling in Vitro Data. *Drug Metab. Dispos.* **2001**, *29*, 1332–1336.
- Tran, T. H.; Von Moltke, L. L.; Venkatakrishnan, K.; Granda, B. W.; Gibbs, M. A.; Obach, R. S.; Harmatz, J. S.; Greenblatt, D. J. Microsomal Protein Concentration Modifies the Apparent Inhibitory Potency of Cyp3a Inhibitors. *Drug Metab. Dispos.* **2002**, *30*, 1441–1445.
- Margolis, J. M.; Obach, R. S. Impact of Nonspecific Binding to Microsomes and Phospholipid on the Inhibition of Cytochrome P4502D6: Implications for Relating in Vitro Inhibition Data to in Vivo Drug Interactions. *Drug Metab. Dispos.* **2003**, *31*, 606–611.
- Riley, R. J.; McGinnity, D. F.; Austin, R. P. A Unified Model for Predicting Human Hepatic, Metabolic Clearance from in Vitro Intrinsic Clearance Data in Hepatocytes and Microsomes. *Drug Metab. Dispos.* **2005**, *33*, 1304–1311.
- Austin, R. P.; Barton, P.; Cockroft, S. L.; Wenlock, M. C.; Riley, R. J. The Influence of Non-Specific Microsomal Binding on Apparent Intrinsic Clearance, and Its Prediction from Physicochemical Properties. *Drug Metab. Dispos.* **2002**, *30*, 1497–1503.
- Van de Waterbeemd, H.; Gifford, E. Admet in silico modelling: Towards Prediction Paradise? *Nat. Rev. Drug Discovery* **2003**, *2*, 192–204.
- Ekins, S.; Boulanger, B.; Swaan, P. W.; Hupcey, M. A. Z. Towards a New Age of Virtual ADME/TOX and Multidimensional Drug Discovery. *J. Comput.-Aided Mol. Des.* **2002**, *16*, 381–401.
- Obach, R. S. Metabolism of Ezlopitant, a Nonpeptidic Substance P Receptor Antagonist, in Liver Microsomes; Enzyme Kinetics, Cytochrome P450 Isoform Identity, and in Vitro–in Vivo Correlation. *Drug Metab. Dispos.* **2000**, *28*, 1069–1076.
- Naritomi, Y.; Terashita, S.; Kimura, S.; Suzuki, A.; Kagayama, A.; Sugiyama, Y. Prediction of Human Hepatic Clearance from in Vivo Animal Experiments and in Vitro Metabolic Studies with Liver Microsomes from Animals and Humans. *Drug Metab. Dispos.* **2001**, *29*, 1316–1324.
- Omega, version 1.8.1; Openeye Scientific Software: Santa Fe, NM, 2005.
- Boström, J.; Greenwood, J. R.; Gottfries, J. Assessing the Performance of Omega with Respect to Retrieving Bioactive Conformations. *J. Mol. Graphics Modell.* **2003**, *21*, 449–462.
- Boström, J. Reproducing the Conformations of Protein-Bound Ligands: A Critical Evaluation of Several Popular Conformational Searching Tools. *J. Comput.-Aided Mol. Des.* **2001**, *15*, 1137–1152.
- Kirchmair, J.; Wolber, G.; Laggner, C.; Langer, T. Comparative Performance Assessment of the Conformational Model Generators Omega and Catalyst: A Large-Scale Survey on the Retrieval of Protein-Bound Ligand Conformations. *J. Chem. Inf. Model.* **2006**, *46*, 1848–1861.
- Catalyst, version 4.11; Accelrys: San Diego, CA, 2006.
- Marvinview, version 4.0.3; Chemaxon: Budapest, Hungary, 2005.
- Williams, J. SciFinder from CAS; Information at the Desktop for Scientists. *Online (Medford, NJ, U. S.)* **1995**, *19*, 60–66.
- Advanced Chemistry Development (ACD/Labs) Software, version 8.14 for Solaris; ACD/Labs: Toronto, ON, Canada, 2006.
- ROCS, version 2.1.1; Openeye Scientific Software: Santa Fe, NM, 2005.
- Grant, J. A.; Gallardo, M. A.; Pickup, B. T. A Fast Method of Molecular Shape Comparison. A Simple Application of a Gaussian Description of Molecular Shape. *J. Comput. Chem.* **1996**, *17*, 1653–1666.
- Austin, R. P.; Barton, P.; Davis, A. M.; Fessey, R. E.; Wenlock, M. C. The Thermodynamics of the Partitioning of Ionizing Molecules between Aqueous Buffers and Phospholipid Membranes. *Pharm. Res.* **2005**, *22*, 1649–1657.
- Herbette, L.; Katz, A. M.; Sturtevant, J. M. Comparisons of the Interaction of Propranolol and Timolol with Model and Biological Membrane Systems. *Mol. Pharmacol.* **1983**, *24*, 259–269.
- Avdeef, A.; Box, K. J.; Comer, J. E. A.; Hibbert, C.; Tam, K. Y. pH-Metric logP 10. Determination of Liposomal Membrane–Water Partition Coefficients of Ionizable Drugs. *Pharm. Res.* **1998**, *15*, 209–215.

CI600221H